Dual Function of Cyk2, a cdc15/PSTPIP Family Protein, in Regulating Actomyosin Ring Dynamics and Septin Distribution

John Lippincott and Rong Li

Department of Cell Biology, Harvard Medical School, Boston, Massachusetts 02115

Abstract. We previously showed that the budding yeast *Saccharomyces cerevisiae* assembles an actomyosin-based ring that undergoes a contraction-like size change during cytokinesis. To learn more about the biochemical composition and activity of this ring, we have characterized the in vivo distribution and function of Cyk2p, a budding yeast protein that exhibits significant sequence similarity to the cdc15/PSTPIP family of cleavage furrow proteins. Video microscopy of cells expressing green fluorescent protein (GFP)-tagged Cyk2p revealed that Cyk2p forms a double ring that coincides with the septins through most of the cell cycle. During cytokinesis, however, the Cyk2 double ring merges with the actomyosin ring and exhibits a contraction-like size change that is dependent on Myo1p. The septin double ring, in contrast, does not undergo the contraction-like size change but the separation between the two rings increases during cytokinesis. These observations suggest that the septin-containing ring is dynamically distinct from the actomyosin ring and that Cyk2p transits between the two types of structures. Gene disruption of *CYK2* does not affect the assembly of the actomyosin ring but results in rapid disassembly of the ring during the contraction phase, leading to incomplete cytokinesis, suggesting that Cyk2p has an important function in modulating the stability of the actomyosin ring during contraction. Overexpression of Cyk2p also blocks cytokinesis, most likely due to a loss of the septins from the bud neck, indicating that Cyk2p may also play a role in regulating the localization of the septins.

Key words: cytokinesis • actin • myosin • septins • yeast

The mechanisms that mediate and control cytokinesis are fundamental to the successful completion of the cell cycle. Despite active research throughout the years, these mechanisms remain elusive. Animal cells divide by cleavage furrow formation and the action of an actomyosin-based contractile ring (for review see Schroeder, 1990; Satterwhite and Pollard, 1992; Fishkind and Wang, 1995). The timing and positioning of the cleavage furrow and contractile ring are crucial for the proper distribution of organelles and genetic information. The mechanochemical activity of the contractile ring is unclear, but it is believed to function in a manner analogous to actin and myosin in muscle. However, the contractile ring exhibits several differences from the sliding actin-myosin filaments in sarcomeres: (*a*) the actin and myosin filaments in the cleavage furrow are not always organized in parallel arrays (Verkhovsky and Borisy, 1993; Maupin et al., 1994); (*b*) there is an intimate association of the contractile ring with the cell membrane (Schroeder, 1990); (*c*) the ring gets smaller without increasing in width, indicating that contractile ring components leave the ring as contraction occurs (Schroeder, 1972); and (*d*) the contractile ring contains components that have not been found in myofibrils (for review see Fishkind and Wang, 1995). Some of these components must contribute to the stability of the contractile ring to ensure its integrity during force generation. It is this complexity which has hampered the study of this critical structure and process.

Cytokinesis studies in the fission yeast *Schizosaccharomyces pombe* have revealed a number of important proteins involved in different aspects of cytokinesis (for review see Chang and Nurse, 1996; Gould and Simanis, 1997). One of these proteins, cdc15p, has been shown to be a component of the actomyosin ring and essential for cytokinesis. cdc15p is a phosphoprotein containing a potential coiled coil domain, PEST sequences, and a carboxy-terminal SH3 domain (Fankhauser et al., 1995). Temperature-sensitive *cdc15* mutant cells exhibit defects in localizing at least two medial ring components, actin and cdc12p, a

Address correspondence to R. Li, Department of Cell Biology, Harvard Medical School, 240 Longwood Ave., Boston, MA 02115. Tel.: (617) 432-0640. Fax: (617) 431-1144. E-mail: rli@hms.harvard.edu

formin family protein, suggesting that cdc15p is involved in the assembly of the actomyosin ring (Fankhauser et al., 1995; Chang et al., 1997). A recent study showed that *cdc15* mutant cells are also unable to accumulate actin patches at the septum (Balasubramanian et al., 1998). Homologues of cdc15p have been found in multicellular organisms, including tapeworm, mouse, and human. The murine homologue, PSTPIP, has recently been shown to be involved in aspects of cytoskeletal activities, including cytokinesis. It localizes to the cleavage furrow, and like cdc15p, blocks cytokinesis when overexpressed in *S. pombe* (Spencer et al., 1997).

In budding yeast, many proteins localize to the bud neck, the site of cell division. Cortical actin patches localize at the bud neck around the time of cell division, although their function is unknown. Another set of neck components involved in cytokinesis are the septins. The septins contain the products of the *CDC3*, *CDC10*, *CDC11*, and *CDC12* genes and are thought to be the major component of the 10-nm neck filaments (for review see Longtine et al., 1996). Mutations in the septin genes lead to defects in cell morphogenesis and cytokinesis. The septins have also been found in the cleavage furrow of animal cells, suggesting that their role in cytokinesis is conserved (Kinoshita et al., 1997). Recently, it was discovered that the budding yeast *Saccharomyces cerevisiae* also utilizes an actomyosin-based ring that exhibits contraction-like size change during cytokinesis (Bi et al., 1998; Lippincott and Li, 1998). In this organism the septins are required for the localization of myosin II to the site of cell division, providing evidence that the septins functionally interact with the actomyosin ring.

So far, only three proteins have been directly implicated in contractile ring activity in budding yeast: Act1p (actin), Myo1p (a myosin II), and Cyk1p (an IQGAP-like protein). Genetic analysis demonstrated that Cyk1p is crucial for the recruitment of actin filaments to the Myo1 ring (Lippincott and Li, 1998). Further study of cytokinesis in budding yeast relies on the identification of additional proteins that interact with the actomyosin ring. In this paper, we describe the characterization of a protein that interacts with both the septin ring and the actomyosin ring. This protein, termed Cyk2p, is a budding yeast homologue of cdc15p. A combination of genetics and video microscopy analyses has revealed important information about the role of Cyk2p in actomyosin ring activity and provided novel insights into the function of the cdc15/PSTPIP family proteins.

Materials and Methods

Media and Genetic Manipulations

Yeast cell culture and genetic techniques were carried out by methods described in Sherman et al. (1974). Yeast extract, peptone, dextrose (YPD)[1] contained 2% glucose, 1% yeast extract, and 2% Bactopeptone (Difco Laboratories, Detroit, MI). YPG contained 2% galactose, 2% raffinose, 1% yeast extract, and 2% Bactopeptone. Synthetic complete media was prepared by the method described in Kaiser et al. (1994).

Plasmid Construction

To construct *CYK2*-expressing plasmids, a DNA fragment containing a 265-bp 5′ sequence and the entire open reading frame (ORF) of *CYK2* was amplified by PCR against yeast genomic DNA. This fragment was digested with PstI (site included in the 5′ primer) and BamHI (site included in the 3′ primer immediately following the coding sequence for the last amino acid), and then cloned between the corresponding sites in pRL72 (a COOH-terminal myc-tagging vector) and pRL73 (a COOH-terminal green fluorescent protein [GFP]-tagging vector) (Lippincott and Li, 1998) to yield pLP1 and pLP2, respectively. pLP2 was digested with SalI and NotI and the fragment containing CYK2–GFP was cloned into the SalI and NotI sites of pRS313 to generate pLP3. The PstI/BamHI fragment used to generate pLP1 was also cloned into bluescript SK at the same sites to yield pLP5. A *CYK2* disruption plasmid, pLP6, was constructed by digesting pLP5 with BglII and StyI, removing 86% of the *CYK2* ORF, blunting both ends, and ligating the vector fragment with the blunted *HIS3* marker gene (Berben et al., 1991). To generate the plasmid that expresses *CYK2* under the control of the *GAL1* promoter, *CYK2* was amplified by PCR against genomic DNA with primers that included the 3′ stop codon, but started immediately downstream of the ATG which follows an in-frame SalI site. This PCR fragment was cloned into pcDNA3.1/v5/His-TOPO (Invitrogen, Carlsbad, CA) to generate pLP21. pLP21 was subsequently digested with SalI, and the *CYK2* fragment was ligated into the SalI site of pRL62, a pRS306 based vector for NH_2-terminal hemagglutinin (HA) tagging of genes under the *GAL1* promoter. Orientation was determined so that the second amino acid of Cyk2 is directly downstream and in-frame with the HA tag.

To construct the septin GFP-expressing plasmid, a DNA fragment containing a 242-bp 5′ sequence and the entire ORF of *CDC12* was amplified by PCR against yeast genomic DNA. This fragment was digested with PstI (site included in the 5′ primer) and BamHI (site included in the 3′ primer immediately following the coding sequence for the last amino acid), and cloned between the corresponding sites in pRL73 to yield pLP17.

To construct the *MYO1* disruption plasmid, bluescript SK was double digested with HindIII and EcoRI, blunted, and then religated to generate pLP10-5. A DNA fragment containing a 226-bp 5′ sequence and the entire ORF of *MYO1* was amplified by PCR against yeast genomic DNA. This fragment was digested with PstI (site included in the 5′ primer) and BamHI (site included in the 3′ primer immediately following the coding sequence for the last amino acid), and then cloned between the corresponding sites in pLP10-5 to yield pLP11. pLP11 was subsequently digested with EcoRV to remove 5,111 bp (88%) of the *MYO1* ORF which was replaced by ligating in the *HIS3* marker gene to generate pRL185.

Strain Construction

All strains used in this study are listed in Table I. To disrupt *CYK2*, pLP6 was digested with EcoRI and XbaI, and then transformed into RLY138 and RLY323 to yield RLY392 and RLY416, respectively. RLY292, the haploid S288c background *Δcyk2* strain, was generated from tetrad dissection of RLY392. *CYK2* gene disruption was confirmed by PCR analysis of the genomic DNA prepared from the His^+ colonies using a 5′ primer corresponding to a sequence within the *CYK2* coding region that is replaced by the *HIS3* marker gene in the disruption allele and a 3′ primer corresponding to a sequence 3′ to the *CYK2* coding region that is not present in pLP6 (data not shown). To generate a strain expressing *CYK2* under the control of the *GAL1* promoter (RLY292), pLP23 was linearized with XcmI and integrated into the *URA3* locus of RLY261. Expression and galactose-specific induction of HA-Cyk2p was confirmed by immunoblot analysis (data not shown). RLY332 (the *Δmyo1* strain) was generated by digesting pRL185 with BamHI and XhoI, and then transforming into the haploid strain RLY8. *MYO1* gene disruption was confirmed by PCR analysis of the genomic DNA prepared from the His^+ colonies using a 5′ primer corresponding to a sequence within the *MYO1* coding region that is replaced by the *HIS3* marker gene in the disruption allele and a 3′ primer corresponding to a sequence 3′ to the *MYO1* coding region that is not present in pRL185 (data not shown). The parental strain of RLY519 contains *Δarp2::TRP1* and *ARP2–GFP*. *ARP2–GFP* is a functional protein as it complements the *Δarp2::TRP1* deficiency (Winter, D., and R. Li, unpublished result). A strain containing tubulin-GFP and Cyk2–GFP was generated by transforming pLP2 into RLY392. The resulting strain was

1. *Abbreviations used in this paper*: Cyk2, cytokinesis 2; GFP, green fluorescent protein; HA, hemagglutinin; ORF, open reading frame; YPD, yeast extract, peptone, dextrose; YPG, yeast extract, peptone, galactose, raffinose.

Table I. Yeast Strains

Name	Genotype	Background	Source
RLY8	*MATa ura3-52 his3-Δ200 leu2-3,112 lys2-801 Δbar1*	S288c	Li lab, Harvard Medical School, Boston, MA
RLY138	*MATa/α ura3-52/ura3-52 his3-Δ200/his3-Δ200 leu2-3,112/leu2-3,112 lys2-801/lys2-801*	S288c	Li lab
RLY261	*MATa ura3-1 his3-11,15 leu2-3,112 trp1-1 ade2-1 Δbar1*	W303	Elion lab, Harvard Medical School
RLY323	*MATa/α ura3-1/ura3-1 his3-11,15/his3-11,15 leu2-3,112/leu2-3,112trp1-1/trp1-1 ade2-1/ade2-1 can1-100/can1-100*	W303	Elion lab
RLY286	*MATa ura3-52 his3-Δ200 leu2-3,112 lys2-801 Δbar1 pCYK2-GFP* (*pLP2*)	S288c	This work
RLY292	*MATa ura3-52 his3-Δ200 leu2-3,112 lys2-801 Δcyk2::HIS3*	S288c	This work
RLY294	*MATa ura3-52 his3-Δ200 leu2-3,112 lys2-801 Δcyk2::HIS3 pCYK2-myc* (*pLP1*)	S288c	This work
RLY332	*MATa ura3-52 his3-Δ200 leu2-3,112 lys2-801 Δbar1 Δmyo1::HIS3*	S288c	This work
RLY370	*MATa ura3-52 his3-Δ200 leu2-3,112 lys2-801 Δbar1 pCDC12-GFP* (*pLP17*)	S288c	This work
RLY392	*MATa/α ura3-52/ura3-52 his3-Δ200/his3-Δ200 leu2-3,112/leu2-3,112 lys2-801/lys2-801 CYK2/Δcyk2::HIS3*	S288c	This work
RLY414	*MATa ura3-52 his3-Δ200 leu2-3,112 lys2-801 Δbar1 Δmyo1::HIS3 pCYK2-GFP* (*pLP2*)	S288c	This work
RLY416	*MATa/α ura3-1/ura3-1 his3-11,15/his3-11,15 leu2-3,112/leu2-3,112trp1-1/trp1-1 ade2-1/ade2-1 can1-100/can1-100 CYK2/Δcyk2::HIS3*	W303	This work
RLY476	*MATa ura3-52 his3-Δ200 leu2-3,112 lys2-801 Δcyk2::HIS3*	S288c	This work
RLY519	*MATa ura3-52 his3-Δ200 leu2-3,112 trp1-1 Δarp2::TRP1 ARP2-GFP::LEU2 pCYK2-GFP* (*pLP3*)	S288c	This work
RLY533	*MATa ura3-52 his3-Δ200 leu2-3,112 lys2-801 Δcyk2::HIS3 Myo1-GFP::URA3*	S288c	This work
RLY534	*MATa ura3-52 his3-Δ200 leu2-3,112 lys2-801 Myo1-GFP::URA3*	S288c	This work
RLY535	*MATa/α ura3-52/ura3-52 his3-Δ200/his3-Δ200 leu2-3,112/leu2-3,112lys2-801/lys2-801 CYK2/Δcyk2::HIS3 MYO1-GFP::URA3*	S288c	This work
RLY536	*MATa ura3-1 his3-11,15 leu2-3,112 trp1-1 ade2-1 Δbar1 GAL1-HA-CYK2::URA3*	W303	This work
RLY569	*MATa ura3-1 his3-11,15 leu2-3,112 trp1-1 ade2-1 Δbar1 GAL1-HA::URA3*	W303	This work
RLY617	*MATa ura3-52 his3-Δ200 leu2-3,112 lys2-801 Δbar1 cdc12-6 pCYK2-myc* (*pLP1*)	S288c	This work
RLY618	*MATa ura3-52 his3-Δ200 leu2-3,112 lys2-801 Δbar1 CDC12 pCYK2-myc* (*pLP1*)	S288c	This work
RLY620	*MATa ura3-52 his3-Δ200 leu2-3,112 lys2-801 Δcyk2::HIS3 pCYK2-GFP* (*pLP2*) *Tub1–GFP::URA3*	S288c	This work

then sporulated and dissected to generate a strain in which the only copy of Cyk2 was Cyk2–GFP. This strain was then transformed with Stu1-linearized pAFS125 (Straight et al., 1997) to generate RLY620.

Zymolyase Treatment

For the experiments shown in Fig. 5, *C* and *D* and Fig. 7 *E*, 5 ml of cells were fixed by the addition of 37% formaldehyde to 5% final concentration and incubation at room temperature for 1 h with gentle agitation, washed twice with PBS and once with 1 M sorbitol in 50 mM KPO_4, pH 7.5. Cells were incubated with 0.2 mg/ml zymolyase 20T (Seikagaku Corp., Tokyo, Japan) in the above sorbitol buffer containing 2 mM DTT for 10 min at 37°C. Typically >90% of the treated cells lost the refractile appearance when observed under a Nikon Labophot-2 microscope with a Plan 40 0.5 ELWD objective (Melville, NY), indicating that cell wall removal was efficient.

Fluorescence Staining of Yeast Cells

Cells grown in YPD were fixed directly in growth media by addition of 37% formaldehyde to 5% final concentration and incubation at room temperature for 1 h with gentle agitation. Cells grown in synthetic media were shifted to growth in YPD for 1 h before fixation because the low pH of the synthetic media resulted in poor fixation. Phalloidin staining was performed as described (Guthrie and Fink, 1991) except that the cells were treated with zymolyase to remove the cell wall after fixation in all of the experiments in this study with the exception of the cells from the 4-h time point in Fig. 7 *B* (in order to show cell morphology). Immunofluorescent staining using either mouse anti-myc (Evan et al., 1985), rabbit anti-Cdc3 (Frazier et al., 1998), or mouse anti-HA primary antibodies and FITC-conjugated or rhodamine-conjugated secondary antibodies (Jackson ImmunoResearch, West Grove, PA) was carried out as described (Drubin et al., 1988). To double stain cells with rhodamine-phalloidin and an antibody, the methanol/acetone treatment was omitted from the immunofluorescence staining procedure. After incubation with the secondary antibody, the cells were incubated with 0.05 μM rhodamine-phalloidin (Molecular Probes, Eugene, OR) for 20–30 min in the dark. The cells were visualized on a Zeiss Axiophot microscope with a HB100 W/Z high-pressure mercury lamp and a Zeiss 100× Plan Neofluar oil immersion objective (Carl Zeiss, Thornwood, NY). Image acquisition was carried out using Northern Exposure (Phase 3 Imaging Systems, Milford, MA).

DiI and Calcofluor Staining

DiI was purchased from Molecular Probes and a 1-mg/ml stock solution was made in 95% EtOH. 1 ml of cells at a density of OD_{600} ~0.3 were pelleted by centrifugation and resuspended gently in 100 μl of DiI stock solution. Cells were incubated for 20 min at 37°C, washed three times with H_2O, and then viewed using a rhodamine filter set. Calcofluor staining was done essentially as previously described (Pringle, 1991). A fluorescent brightener 28 (Sigma, St. Louis, MO) stock solution was prepared in H_2O at 1 mg/ml. Cell pellets prepared as above were resuspended in 100 μl stock solution, incubated 5 min at room temperature, washed three times with H_2O and viewed using a 4′,6-diamidino-2-phenylindole (DAPI) filter set. Serial sections were obtained using wide-field deconvolution three-dimensional microscopy (Agard et al., 1989).

Measurements of Fluorescence Intensity

The average maximum fluorescence intensities presented in Fig. 6 were measured in the following manner: the two dots of fluorescence at the bud neck represent a perpendicular section through the Myo1–GFP ring. WinView 32 software (Princeton Instruments, Trenton, NJ) was used to measure the brightest pixels in both dots (left and right sides of the ring). The brightest pixels were averaged together and the background was subtracted. The background was measured by averaging over 20 separate pixel values located away from the bud neck at each time point. In the case of asymmetrical Myo1–GFP ring contractions, the brightest pixels were not averaged and each dot was considered separately. Intensity profiles (see Fig. 6 *C*) were measured using custom software developed for WinView 1.6.2 (courtesy of A. Mallavarapu, Harvard Medical School, Boston, MA) in the following manner: a line was drawn through the Myo1–GFP ring of a cell image obtained as described below. The intensity values through the thickness of the line (two pixels) were averaged and plotted against the distance of the line. The line drawn through the wild-

type cell neck was 15 pixels (1.23 μm) long and the line drawn through the *Δcyk2* cell neck was 30 pixels (2.46 μm) long.

Time-Lapse Imaging of Cells Expressing GFP-tagged Proteins

Strains expressing GFP-tagged proteins were grown overnight in selective media and placed on agarose pads essentially as described (Waddle et al., 1996). Living cells were imaged at room temperature on an Eclipse E600 microscope with a 100/1.40 oil differential-interference contrast objective (Nikon). Images of Myo1–GFP were collected through a neutral density filter of value 8 every 30 s with 0.8 s of exposure to fluorescent light filtered through a EXHQ450/50 DM480 LP/BA465LP GFP filter set (Chroma, Brattleboro, VT) using a cooled RTE/CCD 782Y Interline camera (Princeton Instruments). The shutter was controlled automatically using a D122 shutter driver (UniBlitz, Rochester, NY) and WinView 1.6.2 software (Princeton Instruments) with custom software (courtesy of A. Mallavarapu). Images of Cyk2–GFP were collected using the same system, every 30 s without a neutral density filter and 0.05-s exposures. Images of Cdc12–GFP were collected using the same setup every 30 s with a neutral density filter of value 4 and a 0.1-s exposure. Cells imaged by the above method usually remain healthy for more than one cell cycle as judged by the rate of bud appearance or growth. Images of Arp2–GFP and Cyk2–GFP in the same cell were also collected every 30 s using the same setup with a neutral density filter of value 8 and a 0.5-s exposure.

Images of tubulin–GFP and Cyk2–GFP in the same cell were collected at room temperature using a Zeiss Axiovert 100 TV microscope through a neutral density filter of value 3 every 30 s with 0.5-s exposure to fluorescent light filtered through a EXHQ450/50 DM480 LP/BA465LP GFP filter set

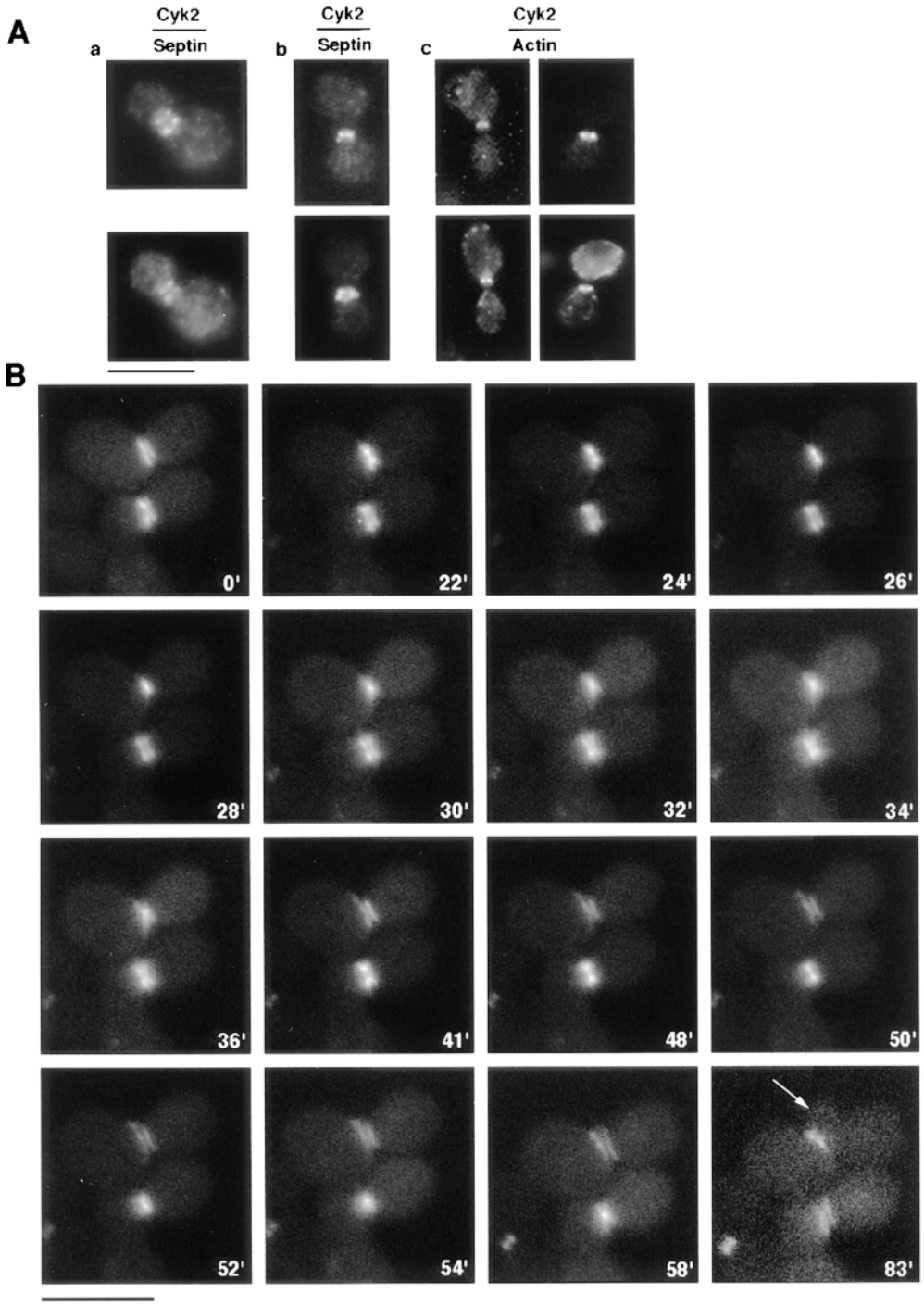

Figure 1. Intracellular localization of Cyk2p. (*A*) RLY-294 (Cyk2-myc–expressing) cells were fixed and double stained with mouse anti-myc and either rabbit anti-Cdc3p (panels *a* and *b*) or rhodamine-phalloidin (panel *c*, two examples shown). (*B*) RLY286 (Cyk2-GFP–expressing) cells were observed by video microscopy as described in Materials and Methods. *Arrow* in the 83′ panel, a new bud. Bars, 10 μm.

(Chroma) using a cooled RTE/CCD 782Y Interline camera (Princeton Instruments). Seven z-sections were acquired at each timepoint through a 3-μm range using a Ludl z-motor controlled by PHAT-Lapse software (courtesy of A. Mallavarapu) for WinView 32 (Princeton Instruments) and then flattened into a single image using PHAT-Lapse software.

Results

We had previously shown that *Saccharomyces cerevisiae* contains an actomyosin-based ring at the bud neck which is important for cytokinesis (Lippincott and Li, 1998). This ring undergoes a contraction-like size change during cytokinesis. For convenience, we will refer to this event as contraction throughout the paper even though rigorous tests of the actual mechanism are still lacking. To further understand the regulation and mechanism of function of this ring, it is important to identify additional ring components. To this effect we cloned an ORF found in the yeast genomic database whose predicted amino acid sequence shows significant similarity to the *S. pombe* cdc15 protein (Fankhauser et al., 1995). cdc15 is a component of the medial ring in fission yeast and is required for the completion of cytokinesis and accumulation of actin patches to the septum (Fankhauser et al., 1995; Balasubramanian et al., 1998). We have named the cdc15 homologue of budding yeast Cyk2 (for cytokinesis 2) because of its involvement in cytokinesis (see below). A sequence alignment between this ORF and cdc15 was previously published (Fankhauser et al., 1995) and showed that the *S. cerevisiae* cdc15-like protein also possesses a potential coiled-coil region and a COOH-terminal SH3 domain.

Cyk2p Shuttles between the Septin and the Actomyosin Rings

To test whether Cyk2p is indeed a component of the actomyosin ring in budding yeast cells, we tagged the protein at the COOH terminus with either six myc epitopes or GFP. Both of these constructs complemented the null phenotypes (see below and data not shown). Cyk2p was found to localize to the mother–bud junction, usually appearing as a double ring around the neck. In most cells, the Cyk2 double ring colocalized with the septin double ring (Fig. 1 *A*, panel *a*), but in a small fraction of anaphase cells, Cyk2p localizes to a single ring "sandwiched" between the septin rings (Fig. 1 *A*, panel *b*). Because the actomyosin ring usually appears as a single ring in between the septin rings (Lippincott and Li, 1998), we examined whether Cyk2p sometimes colocalizes with the actin ring. Double staining of Cyk2p and actin showed that in anaphase cells where actin filaments had been recruited to the Myo1 ring, the Cyk2 ring often appeared as a single ring colocalizing with the actin ring (Fig. 1 *A*, panel *c*).

The above immunolocalization results suggest that Cyk2p shifts from the septin rings to the actomyosin ring sometime during anaphase. To further investigate this possibility, we examined the in vivo changes in Cyk2p localization by time-lapse video microscopy on living cells expressing Cyk2–GFP. The Cyk2–GFP ring was found in cells with buds of all sizes (data not shown). Fig. 1 *B* shows a time-lapse sequence of Cyk2–GFP localization during one cell cycle. At time 0, Cyk2–GFP was found to localize to a double ring at the neck of two large budded cells. At 24′ (*top*) and 50′ (*bottom*) the Cyk2 double rings appeared to have merged into a single ring. Within the next two minutes, the single ring started to decrease in diameter (Fig. 1 *B*, *24–28′*, *top*; *50–54′*, *bottom*), similar to the contraction-like morphological change of the Myo1 ring observed at cytokinesis (Lippincott and Li, 1998). In contrast to the Myo1 ring which shrinks to a single dot and then disappears, the Cyk2 fluorescence did not disappear, but spread out around the neck area (Fig. 1 *B*, *30–36′*, *top*). This spreading resulted in the reformation of a Cyk2 double ring, half of which resided in the mother, and the other in the daughter (Fig. 1 *B*, *41′*, *top*). One of the Cyk2 rings extended on one side toward the future bud site while it was disappearing from the old bud site (Fig. 1 *B*, *41–58′*, *top*), and eventually formed a new ring as the new bud grew out (*83′*, *arrow* indicates new bud).

To further characterize the timing of Cyk2p localization to the actomyosin ring with respect to spindle and actin dynamics, strains were constructed which coexpressed either Cyk2–GFP and tubulin–GFP or Cyk2–GFP and Arp2–GFP, a component of cortical actin patches. Fig. 2 *A* shows a time-lapse sequence which demonstrates that the Cyk2p double ring merged to a single ring after the completion of spindle elongation (compare *14–22′*). The contraction of the Cyk2 single ring follows (Fig. 2 *A*, *26–32′*), during which the spindle breaks down. Fig. 2 *B* shows a

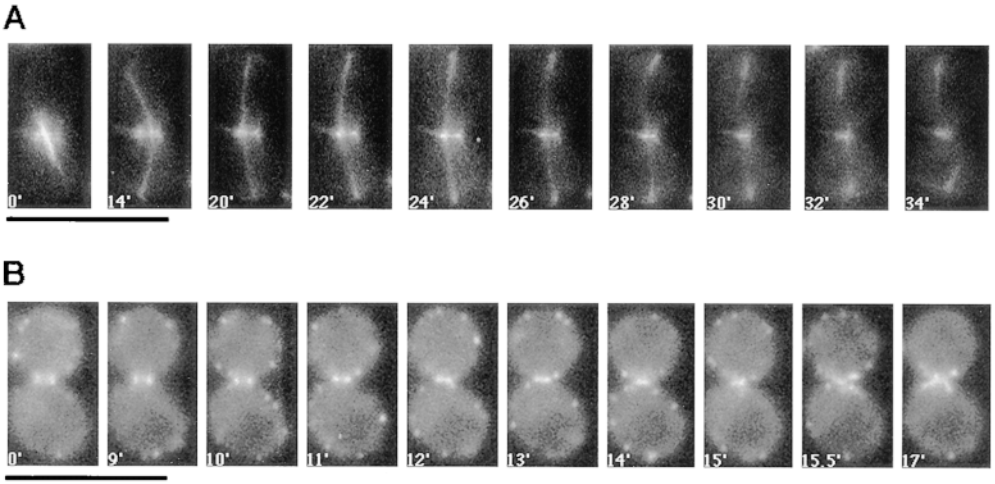

Figure 2. The dynamics of the Cyk2 ring in relation to those of the spindle and cortical actin patches. RLY620 (tubulin-GFP and Cyk2-GFP–expressing) cells (*A*) or RLY519 (Arp2–GFP and Cyk2-GFP–expressing) cells (*B*) were observed by video microscopy as described in Materials and Methods. Bars, 10 μm.

time-lapse sequence which demonstrates that actin patches accumulate at the bud neck at the end of Cyk2–GFP ring contraction (compare actin patch distribution in frames *11–15′* with that in frames *15.5′* and *17′*).

The Septins Are Not Components of the Contractile Ring

To differentiate the localization of Cyk2p from that of the septins, we also examined the in vivo changes in septin localization in cells expressing the COOH-terminal GFP-tagged Cdc12p. The Cdc12–GFP construct complements the null (data not shown) and shows a Cdc12 localization similar to that described previously for the septins (Haarer and Pringle, 1987). Time-lapse video microscopy of Cdc12-GFP–expressing cells revealed that the septin double rings did not merge into a single ring, but rather they moved further apart late in the cell cycle (Fig. 3, *3–4′*). The septin rings never shrank like the Cyk2 or Myo1 ring, suggesting that they are not part of the contractile apparatus. Like Cyk2p, subsequent to cell separation individual septin rings were seen to elongate at one end, mark the new bud site and completely delocalize from the old site as the new bud emerged (Fig. 3, *17–29′*, *bottom ring*). These observations suggest that the septin rings are structurally distinct from the actomyosin ring and that the merging of the Cyk2 double ring to a single ring is not a non-specific consequence of tightening of the neck cortex during cytokinesis.

The Cyk2 Ring Is Disrupted by a Septin Mutation

Because Cyk2p colocalizes with the septins in the early part of the cell cycle, the possibility exists that septins may be required for the assembly and maintenance of the Cyk2 ring. To test this possibility, the Cyk2-myc–expressing construct was introduced into a *cdc12-6* (Kim et al., 1991) mutant strain. The cells were cultured at 23°C, and then shifted to growth at 37°C, the nonpermissive temperature. As expected, the septin ring was lost in >99% of the mutant cells 30 min after the temperature shift (Table II). The Cyk2 ring was also absent in >99% of these cells. There was only a small drop in the fraction of the septin ring-containing or Cyk2 ring-containing cells in the wild-type culture shifted to 37°C (Table II), suggesting that the disappearance of the septin and Cyk2p rings in the mutant culture was not simply due to the temperature shift. This result suggests that the septins play an important role in the assembly and maintenance of the Cyk2 ring. Cyk2p, however, is not required for septin ring localization (see below).

Table II. The Cyk2 Ring Is Abolished by a Septin Mutation

	Percent with a septin ring	Percent with a Cyk2 ring
CDC12 at 23°C	73.5	54.5
CDC12 at 37°C	58	35.5
cdc12-6 at 23°C	44	33.5
cdc12-6 at 37°C	0	0

RLY618 (Cyk2-myc–expressing; *CDC12*) and RLY617 (Cyk2-myc–expressing; *cdc12-6*) cells were grown overnight at 23°C. Half of the cells were maintained at 23°C, and the other half were shifted to growth at 37°C for 30 min, fixed, and then stained with anti-myc and anti-Cdc3 antibodies. Fields of cells were first counted in the phase channel. The number of cells within the same field that had a septin ring or a Cyk2 ring was counted in the appropriate fluorescence channel. The resultant numbers from the counting in the fluorescence channels were divided by the total cell number counted in the phase channel to give percent of cells with a septin ring or percent of cells with a Cyk2 ring. 300–600 cells were counted for each sample.

The Effect of MYO1 Gene Disruption on the Dynamics of the Cyk2-containing Ring

Because the Cyk2 ring merges with the actomyosin ring and exhibits a contraction-like size change late in the cell cycle, we tested whether the dynamics of the Cyk2-containing ring are dependent on Myo1p. The Cyk2–GFP construct was introduced into a *Δmyo1* strain. The *Δmyo1* cells are viable but exhibit severe defects in cytokinesis and colony growth (Watts et al., 1987) (Lippincott, J., and R. Li, unpublished result). Cyk2p is able to localize properly in *Δmyo1* cells through most of the cell cycle, indicating that the normal localization of Cyk2p is not dependent on Myo1p (Fig. 4, *20′* and data not shown). However, in large-budded cells, after the Cyk2 double rings merged into a single ring, the ring broke into small pieces without undergoing the contraction-like size change (Fig. 4, *32–43′*). This result suggests that Myo1p is required for maintaining the integrity and/or contraction of the Cyk2 ring during cytokinesis.

CYK2 Gene Disruption Results in a Cytokinesis Defect

The results described above indicate that Cyk2p is a component of the bud neck and is intimately associated with the actomyosin ring during cytokinesis. To further inves-

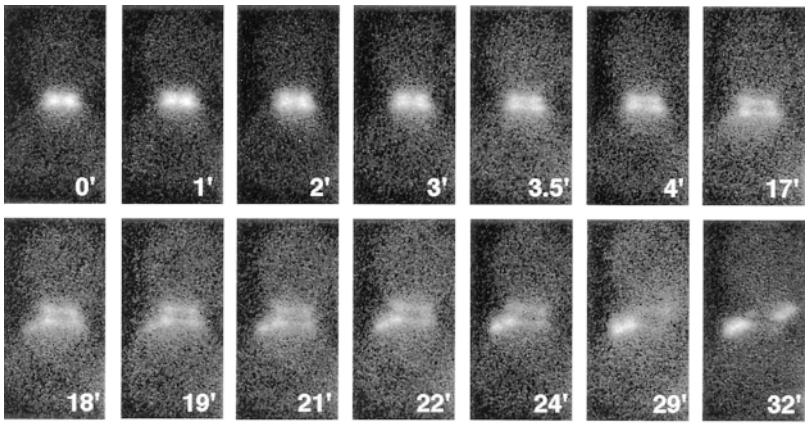

Figure 3. The in vivo dynamics of the septin rings. RLY370 (Cdc12-GFP–expressing) cells were observed by video microscopy as described in Materials and Methods. Bar, 10 μm.

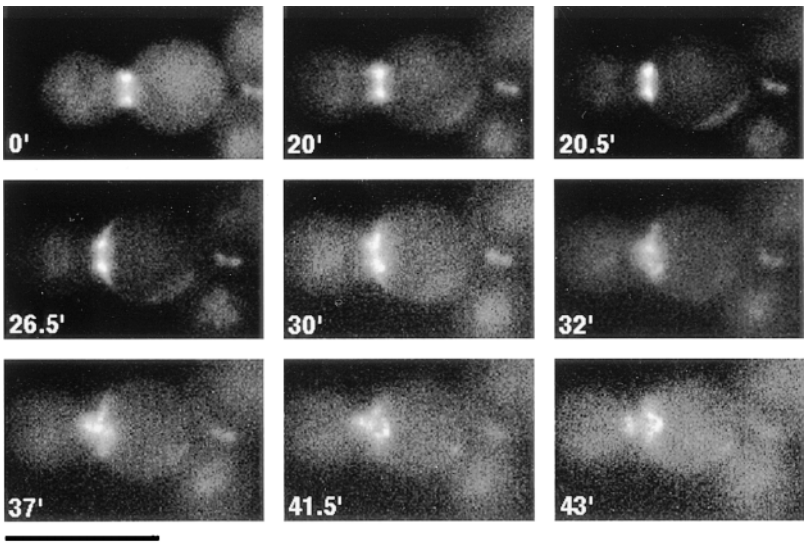

Figure 4. The in vivo dynamics of Cyk2p-containing structure in *Δmyo1* cells. RLY414 (Cyk2-GFP–expressing, *Δmyo1*) cells were observed by video microscopy as described in Materials and Methods. Bar, 10 μm.

tigate the involvement of Cyk2p in cytokinesis, we constructed a null allele of *CYK2* by deleting 86% of the *CYK2* ORF. Because the phenotypes of many cytoskeletal mutants vary significantly between different genetic backgrounds, we disrupted the *CYK2* gene in two commonly studied strain backgrounds: W303 and S288c. Tetrad analysis of a heterozygous diploid *Δcyk2* strain in the W303 genetic background was performed. When the tetrads were grown at room temperature (~23°C), 45% of the *Δcyk2* spores were able to grow into colonies, but the growth of these colonies was much slower than that of the wild-type spores (Fig. 5 *A*, *top left*, two large colonies in each tetrad were His^- and wild type). When the tetrads were dissected and incubated at 30°C, 79 out of 80 *Δcyk2* spores were incapable of small colony formation (Fig. 5 *A*, *bottom left*). Microscopic analysis of the noncolony-forming spores revealed that these *Δcyk2* spores were able to germinate and proceed through a number of cell cycles before lysing as a small chain (Fig. 5 *B*). Many of the cells in the viable colonies were also in chains or clumps.

It is worth noting that these viable *Δcyk2* colonies greatly improved their growth rate and cell morphology after several rounds of streaking on YPD plates, suggesting that these cells somehow adapted or accumulated suppressor mutations. To distinguish between these possibilities, a growth-improved *Δcyk2* strain was backcrossed to the parental wild-type strain. From 12 tetrads, 11 of the 24 (46%) *Δcyk2* spores grew into colonies that were phenotypically indistinguishable from the growth-improved *Δcyk2* colonies. Of the remaining 13 *Δcyk2* spores, six did not grow into visible colonies and seven grew into colonies that were much smaller than wild-type and contained cells with the chain morphology. These results are consistent with a single, unlinked, suppressor mutation which greatly improves the growth of *Δcyk2* cells. No phenotype was observed for $Cyk2^+$ cells that contained this suppressor mutation. In the more robust S288c strain background, *Δcyk2* spores were able to form colonies at 30°C but not at 37°C (Fig. 5 *A*, *right*), although chains or clumps of cells exist in colonies grown at 30°C. The neck of *Δcyk2* cells are often two to three times as wide as the wild-type cells in both strain backgrounds (see Fig. 6). To avoid suppressor mutations, we mostly worked with S288c colonies that freshly came from a tetrad plate cultured at room temperature.

The chains or clumps of cells that were seen in *Δcyk2* colonies could arise from either a cytokinesis defect or a cell separation defect. To distinguish between these possibilities, both wild-type and *Δcyk2* cells in the S288c background were grown for 8 h at 37°C and samples were taken and fixed every 2 h. Each sample was treated with zymolyase to remove the cell wall and cell number per milliliter was determined using a hemacytometer. From the 4-h time point on, the *Δcyk2* cell number did not significantly increase and the cells remained as clumps and chains after the zymolyase treatment, while the wild-type cell number increased exponentially during this time frame (Fig. 5 *C*). The optical density of the *Δcyk2* culture increased at a wild-type rate indicating that the two cultures grew at approximately the same rate (Fig. 5 *D*). Thus, *Δcyk2* cells exhibit a cytokinesis defect defined by the criteria previously described (Hartwell, 1971).

A second experiment was performed to confirm that *Δcyk2* cells display a cytokinesis defect at the nonpermissive temperature. *Δcyk2* cells in the S288c background grown at room temperature were shifted to 37°C for 4 h and stained with either calcofluor (a chitin-specific fluorescent dye) or DiI (cytoplasmic membrane-specific fluorescent dye). The stained cells were observed by serial optical sectioning using wide-field deconvolution three-dimensional microscopy (Agard et al., 1989). Fig. 5 *E* (*top*) shows a series of 400-nm sections through a typical clump of *Δcyk2* cells after DiI staining. By looking through the series it was clear that the cytoplasm is connected between all four cell bodies, whereas in a wild-type control cell that has completed cytokinesis, no cytoplasm connection was observed at any focal plane (Fig. 5 *E*, *bottom*). Calcofluor staining of *Δcyk2* cells confirmed that a septum had failed to form between two cell bodies before the next round of budding (Fig. 5 *F*).

Because the *cdc15* mutation affects both the proper formation of the actin ring and the accumulation of actin patches at the septum in *S. pombe* (Balasubramanian et al.,

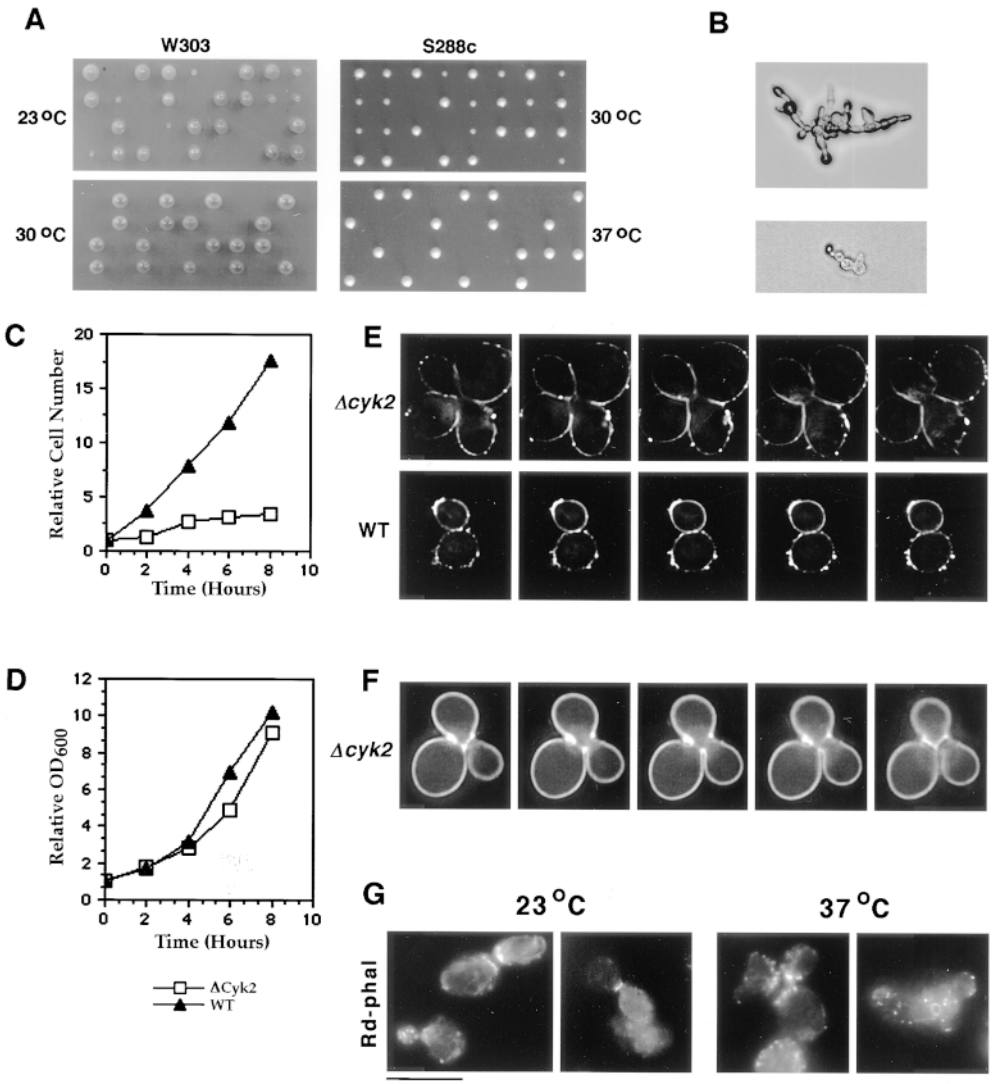

Figure 5. Cyk2p is important for cytokinesis. (*A*) Tetrad analysis of diploid strains heterozygous for the *Δcyk2* mutation (*left panels*: RLY-392, W303 background; *right panels*: RLY416, S288c background). Tetrads were dissected and incubated at either 23°, 30°, or 37°C as indicated. (*B*) Two examples of *Δcyk2* microcolonies which were unable to grow into visible colonies. (*C* and *D*) RLY292 (*Δcyk2*) or RLY8 (wild-type) cells were grown overnight at 23°C and then shifted to 37°C for 8 h. Samples were taken and fixed every 2 h. The cells were either treated with zymolyase and counted on a hemacytometer as described in Materials and Methods (*C*) or subjected to OD_{600} measurements (*D*). The resultant cell concentration or OD_{600} at each time point was divided by that at time 0 to give relative cell number or relative OD_{600}, respectively, and plotted over time. (*E* and *F*) RLY292 (*top panels* in *E* and *F*) or RLY8 (*bottom panels* in *E*) cells were grown overnight at 23°C, shifted to 37°C for 4 h, and then stained with DiI (*E*) or calcofluor (*F*) as described in Materials and Methods. Optical sections were taken using wide-field deconvolution three-dimensional microscopy (Agard et al., 1989). The top panels (*E*) are a series of 400-nm sections, the bottom panels in *E* and those in *F* are a series of 200-nm sections. (*G*) RLY292 cells were grown overnight in YPD at 23°C and then shifted to 37°C. Samples were fixed before the shift and at 4 h after the shift and stained with rhodamine-phalloidin as described in Materials and Methods. Bar, 10 μm.

1998), we examined actin structures in *Δcyk2* cells (Fig. 5 *G*). S288c *Δcyk2* cells were grown at 23° and at 37°C for 4 h, fixed, and then stained for F-actin with rhodamine-phalloidin. At both the permissive and nonpermissive temperatures actin patches polarized properly in small-budded cells and accumulated at the septum in dividing cells (Fig. 5 *G*, *23°C* and *37°C*, *left panels*). The cell in the latter panel has two buds, both of which have patches accumulated at the septum). Actin rings were also able to form in the *Δcyk2* cells and are indistinguishable from those seen in wild-type cells (Fig. 5 *G*, *23°C* and *37°C*, *right panels*). Therefore, unlike cdc15p, Cyk2p does not appear to be required for the normal distribution of actin filaments in the cell. The Myo1 ring also forms properly in *Δcyk2* cells at both the permissive (Fig. 6) and nonpermissive temperature (data not shown), suggesting that Cyk2p is not required for the formation of the contractile ring.

Cyk2p Is Important for the Stabilization of Myo1 Ring during Contraction

Because Cyk2p appears to associate with the actomyosin ring during cytokinesis, it is possible that Cyk2p is important for the contraction of the ring. To test this hypothesis, we introduced Myo1–GFP into the S288c or W303 diploid strains heterozygous for the *Δcyk2* mutation and dissected tetrads. Movies were made of Myo1–GFP in Cyk2-null cells as soon as possible after tetrad dissection (2 d) to avoid suppressor accumulation. Fig. 6 *A*, panel *a* shows Myo1 ring contraction in a typical wild-type cell. The ring appeared to shrink evenly down to a dot in the middle of the bud neck without losing fluorescent intensity (Fig. 6 *A*, panel *a*, *0–3′*). The Myo1 ring was also able to contract in the absence of Cyk2p, but the contraction was clearly aberrant. In contrast to the Myo1 rings observed in wild-type cells, the Myo1 ring in *Δcyk2* cells (all cells observed in

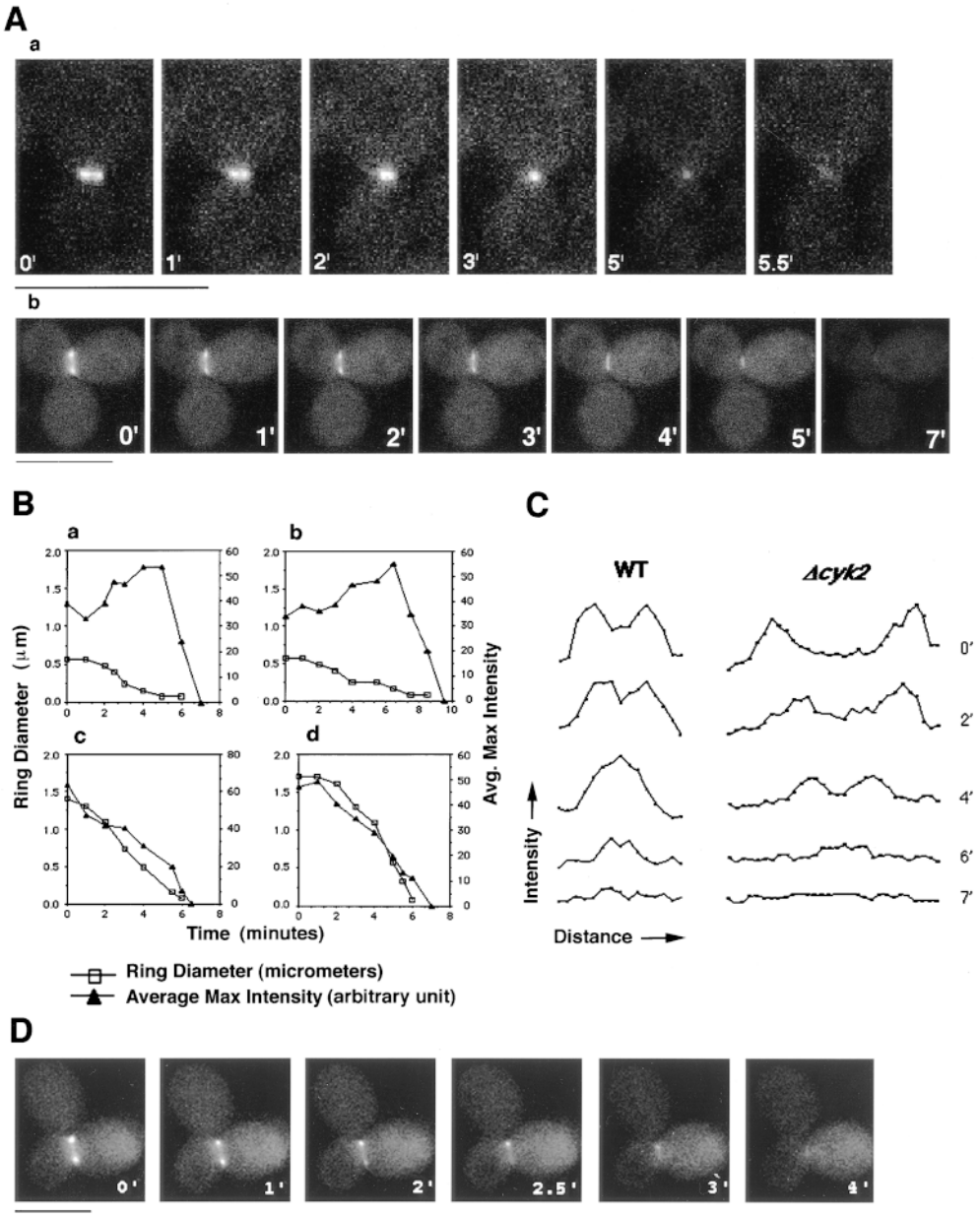

Figure 6. Abnormal contraction of the Myo1 ring in *ΔCTK2* cells. (*A*) RLY534 (panel *a*, Myo1-GFP–expressing, wild-type) or RLY533 (panel *b*, Myo1-GFP–expressing, *Δcyk2*) cells were observed by video microscopy as described in Materials and Methods. (panel *a*) Time-lapse sequence in a typical wild-type cell; (panel *b*) time-lapse sequence in a typical *Δcyk2* cell whose Myo1 ring appeared symmetrical. (*B*) The diameter and average maximum intensity of Myo1 rings in RLY534 and RLY-533 cells were measured using WinView 32 software (Princeton Instruments) as described in Materials and Methods. The measurements were then plotted as a function of time. (panels *a* and *b*) show the results for two typical RLY534 cells and (panels *c* and *d*) for two typical RLY533 cells. (*C*) A line was drawn through the Myo1 ring of a typical RLY534 (*left*) or RLY533 (*right*) cell at each of the indicated time points and pixel intensity values along the line were obtained as described in Materials and Methods. The measurements were then plotted against distance along the line. (*D*) A typical RLY533 cell whose Myo1 ring appeared asymmetrical. Bars, 10 μm.

both backgrounds) appeared to lose width and intensity during contraction (Fig. 6 *A*, panel *b* and Fig. 6 *D*).

Measurements of the maximum fluorescence intensity of the Myo1 ring, which approximates the intensity of the pixel in focus, were taken during Myo1 ring contraction in both wild-type and *Δcyk2* cells. In the wild-type cells the intensity of the Myo1 ring increased as the ring contracted and then decreased drastically after contraction was complete (Fig. 6 *B*, panels *a* and *b* are two typical wild-type cells). In contrast, the intensity of the Myo1 ring in *Δcyk2* cells decreased steadily and rapidly as soon as contraction started (Fig. 6 *B*, panels *c* and *d* are two typical examples). Another way to quantify the difference between the Myo1 ring in wild-type and in *Δcyk2* cells was to obtain intensity profiles along a line cutting across the ring and bud neck. The intensity profile of a typical wild-type cell demonstrates that the Myo1 ring maintained intensity as the two fluorescence peaks at the two sides of the neck moved closer to each other (Fig. 6 *C*, *WT*, *0–4′*). In *Δcyk2* cells, however, the Myo1 ring decreases in intensity as the fluorescence peaks move together (Fig. 6 *C*, *Δcyk2*, *0–6′*). The ability to observe two fluorescence peaks moving together in *Δcyk2* cells also suggests that the narrowing of the ring results from contraction rather than ring subunits diffusing away.

The duration of contraction in the *Δcyk2* cells was roughly the same as that in the wild-type cells. Because the necks of *Δcyk2* cells are up to three times as large in diameter as the wild-type cells, the rate of contraction in the former must be faster than in the latter. Indeed, the rate of contraction was estimated to be 0.26 μm/min (eight cells averaged, $\sigma_{n-1} = 0.119$) in *Δcyk2* cells and 0.10 μm/min (eight cells averaged, $\sigma_{n-1} = 0.039$) in the wild-type cells. Some *Δcyk2* cells had necks similar in size to those in wild-type cells, yet ring contraction was still faster in the mutant cells (data not shown), indicating that the faster contrac-

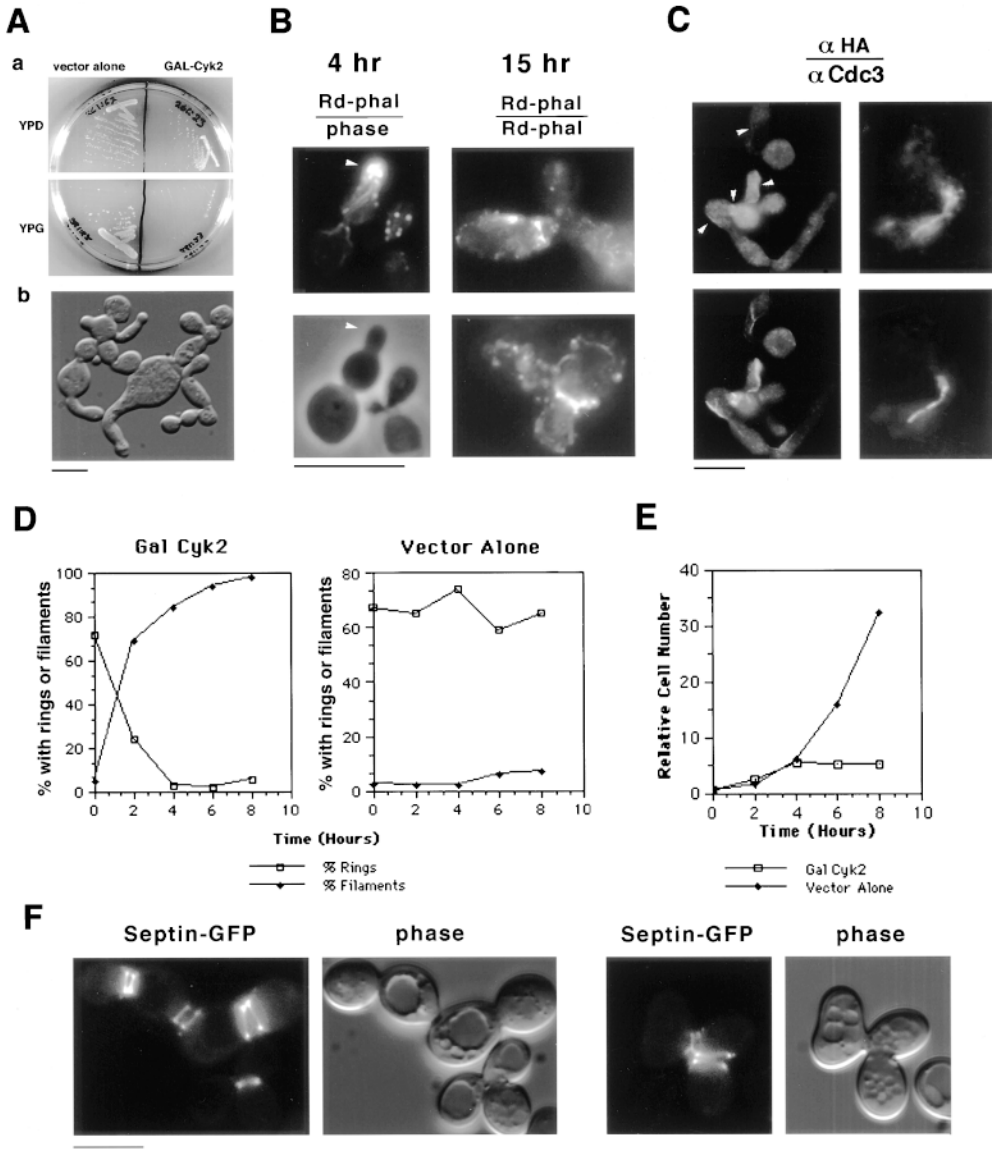

Figure 7. Overexpression of Cyk2p results in an aberrant distribution of the septins and a cytokinesis defect. (*A*, panel *a*) RLY536 (GAL1-HA-CYK2) or RLY569 (vector control) cells were struck out on either YPD or YPG and grown for 3 d at 23°C. (*A*, panel *b*) RLY536 was grown overnight at 23°C in YP-raffinose media. Galactose was added to 2% at time 0 and cells were allowed to grow another 15 h at 23°C. Samples were taken every 2 h up to 8 h and then again at 15 h and fixed. Shown is a phase image of cells from the 8-h timepoint. (*B*) Cells from the 4- and 15-h time points were stained with rhodamine-phalloidin as described in Materials and Methods. (*C*) The fixed RLY536 cells from the 8-h time point were double stained with either mouse anti-HA (*top*) or rabbit anti-Cdc3 (*bottom*) antibodies. (*D*) The RLY536 (*left*) and RLY569 (*right*) cells from each time point of the experiment in *A*, panel *b* were counted by the following method: fields of cells were first counted in the phase channel; the number of cells within the same field that had a septin ring around the bud neck or aberrant septin filaments were then counted in the fluorescent channel. The resultant numbers from the fluorescent channel were divided by the total cell number from the phase channel to give percent cells with septin rings or with aberrant septin filaments. These numbers were plotted as a function of time as shown (200–500 cells were counted for each sample). (*E*) A sample of the RLY536 and RLY569 cells from each time point of the experiment in *A*, panel *b* were treated with zymolyase as described in Materials and Methods and counted on a hemacytometer. The resultant cell concentration at each time point was divided by that at time 0 to give relative cell number and then plotted over time. (*F*) Representative images of GFP fluorescence in RLY476 (Cdc12-GFP–expressing, *Δcyk2*) cells were captured using the setup for time-lapse imaging as described in Materials and Methods. Bars, 10 μm.

tion seen in *Δcyk2* cells was not due to the larger necks observed. Unlike in the wild-type cells, in *Δcyk2* cells after contraction, it was often possible to see vesicle movement through the bud neck by Nomarski imaging indicating that cytokinesis failed to occur. These results suggest that Cyk2p is important for maintaining the stability of the Myo1 ring during contraction, and this defect is likely to be the cause of the cytokinesis failure in *Δcyk2* cells.

In some *Δcyk2* cells (seven out of 10 cells observed in the S288c background, but none in the W303 background), only one of the dots moved and the intensity of the moving dot faded much quicker than the opposite side of the ring (Fig. 6 *D*), suggesting that disassembly occurred asymmetrically. Because the fluorescence peak was abruptly lost on one side, it was difficult to distinguish whether the shortening of the Myo1–GFP "band" from one side was due to asymmetrical contraction or asymmetrical disassembly.

Cyk2p Plays a Role in Regulating Septin Localization

In *S. pombe*, overexpression of cdc15p results in the formation of actin rings in G2 arrested cells and prolonged overexpression of cdc15p inhibits actin ring formation and blocks septation (Fankhauser et al., 1995). To examine the effect of Cyk2p overexpression, we constructed a strain carrying a single integrated copy of *CYK2* tagged with hemagglutinin (HA) epitope under the control of the galactose

inducible *GAL1* promoter. Overexpression of Cyk2p is lethal as cells containing this construct grow on glucose but not galactose-containing media (Fig. 7 *A*, panel *a*). This detrimental effect was not due to the HA tag because the vector alone did not affect growth on galactose media and the HA-Cyk2p complements the null mutation when expressed under the *CYK2* promoter (data not shown). Cells overexpressing Cyk2p adopted chain-like morphology and contained long hyperpolarized buds (Fig. 7 *A*, panel *b*) similar to those seen in septin mutants (Longtine et al., 1996).

To examine the effect of Cyk2p overexpression on actin structures, cells were grown in the presence of galactose for up to 15 h and stained for actin with rhodamine-phalloidin. At time 0, cells contained normal actin structures (data not shown). By 4 h, many cells became hyperpolarized with elongated buds and actin patches were concentrated at the tips of hyperpolarized buds (Fig. 7 *B*, *4 hr*, *arrowhead* indicates elongated bud). Actin rings were not observed in preanaphase cells, suggesting that unlike cdc15 in *S. pombe*, overexpression of Cyk2p does not induce premature actin ring formation (data not shown). After 15 h, however, F-actin aggregates were seen at the bud neck in a small population of cells (~5%) (Fig 7 *B*, *15 h*) and well-organized actin rings were not observed. Thus, prolonged overexpression of Cyk2p may have a similar effect on actin ring formation as seen with prolonged overexpression of cdc15p in *S. pombe*.

Because the cells containing overexpressed Cyk2p exhibit a morphology typical of septin mutants, we determined whether septin organization was affected by Cyk2p overexpression. Cells were grown in galactose-containing media for various amounts of time were fixed and stained for septins (Cdc3) and HA-Cyk2p. Cells overexpressing Cyk2p for 8 h did not contain normal septin rings localized at the bud neck. Long aberrant septin filaments were seen in most of the Cyk2p overexpressing cells (Fig 7 *C*, *bottom*), but rarely in cells containing vector alone (data not shown). Some of these aberrant septin filaments clearly contained HA-Cyk2 (Fig. 7 *C*, *top*, *arrowheads* in *left panel* indicate faint Cyk2p filaments). Fig. 7 *D* shows that the percentage of cells containing aberrant filaments increased proportionally to the number of cells that had lost septin rings from the bud neck. To quantify the apparent cytokinesis defect, the fixed cells from each time point were removed of the cell wall by zymolyase treatment and the resulting spheroplast concentration was determined by cell counting. Although the cell number of the wild type increased exponentially, the cell number of the Cyk2p overexpressing cells plateaued at 4 h, the same time point when most of the cells had lost the septin ring from the bud neck (Fig. 7 *E*). This result suggests that overexpression of Cyk2p results in a loss of septin localization from the bud neck which correlates with an inability to carry out cytokinesis. The appearance of the aberrant septin filaments may be a consequence of the loss of the normal septin structures (see Discussion).

Consistent with an ability of Cyk2 to delocalize the septins, in ~50% of the *Δcyk2* cells that expressed Cdc12–GFP, the septin rings were formed at the new bud neck without delocalizing from the old bud neck, resulting in chains of cells that contained multiple septin rings (Fig. 7 *F*).

Discussion

Cyk2p Shuttles between the Septin Ring and the Actomyosin Ring

In this paper, we first described time-lapse analysis of the in vivo dynamics of Cyk2p localization in comparison with those of the septins and Myo1p using strains expressing GFP-tagged proteins. Fig. 8 *A* depicts the localization pattern of these three proteins before (*top*), during (*middle*), and after (*bottom*) cytokinesis. The Cyk2p-containing rings appear indistinguishable from the septin rings through most of the cell cycle, but just before cytokinesis, the Cyk2 double rings merge into a single ring that coincides with the Myo1p-containing ring. The Cyk2 single ring then shrinks into a bright dot, suggesting that it is part of the actomyosin contractile ring during cytokinesis. The septins, on the other hand, maintain the appearance of a pair of rings with the same diameter, but they grew further apart

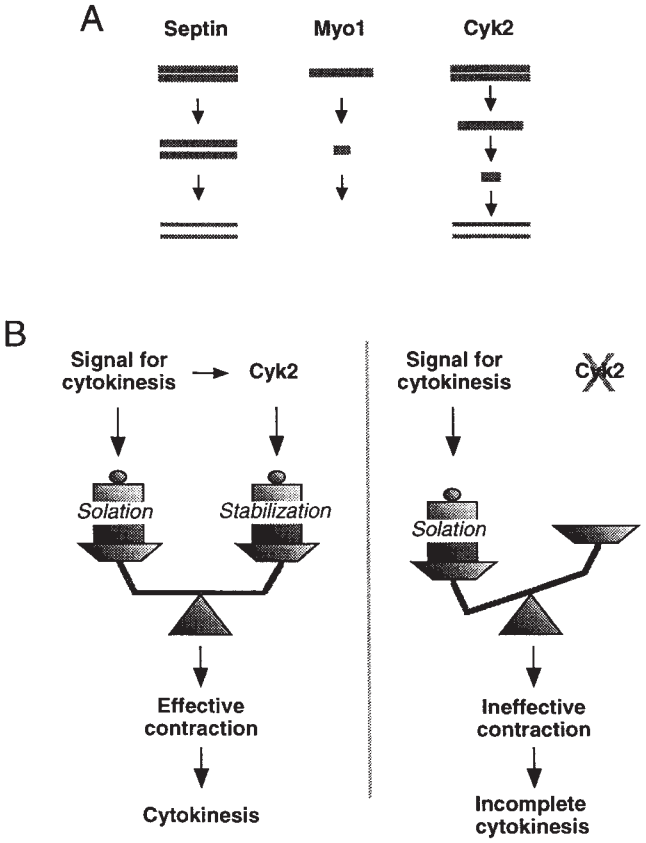

Figure 8. (*A*) A schematic comparison of changes in the morphology of the rings that contain septin, Myo1p, or Cyk2p before (*top*), during (*middle*), and after (*bottom*) cytokinesis. (*B*) A model explaining the role of Cyk2p during the contraction of the actomyosin ring. In wild-type cells (*left*), the cell cycle signal for cytokinesis triggers the solation of the actomyosin ring as well as the association of Cyk2p with actomyosin ring. Effective contraction and completion of cytokinesis result from a balance between the solation activity and the Cyk2p-dependent stabilization of the ring. In *Δcyk2* cells (*right*), the solation is not balanced by the Cyk2p-dependent stabilization, leading to aberrant and ineffective contraction and hence incomplete cytokinesis.

around the time of cytokinesis. Although Myo1p disappears rapidly from the neck region after contraction, Cyk2p redistributes back to two faint rings, whose appearance and location are again indistinguishable from those of the septin rings. At the beginning of the next cell cycle, both the Cyk2 and the septin rings migrate laterally (for axially budding cells) to the incipient bud site by an unknown mechanism.

Further support of the ability of Cyk2p to associate with the septins came from the observations that Cyk2p colocalizes with the aberrant septin filaments which are induced by Cyk2p overexpression and do not contain Myo1p or actin (data not shown), and that the localization of Cyk2p is dependent on the septins (Table II). The conclusion that Cyk2p "hops" onto the Myo1 ring at cytokinesis is also supported by the finding that in *Δmyo1* cells, the Cyk2 ring forms and maintains a normal morphology until the end of the cell cycle when it abruptly breaks, suggesting that its integrity is dependent on Myo1p only at that point. The septin-containing structure has distinct dynamic behaviors from the actomyosin ring. Some interaction must occur between the two structures because the septins are required for the maintenance of the actomyosin ring (Lippincott and Li, 1998) and because the dynamics of the two ring structures are likely to be coordinated during cytokinesis. Cyk2p, which seems to transit between the two structures, could mediate the communication between the septins and the actomyosin ring. Alternatively, Cyk2p could have two independent functions when associated with each structure. We have noticed that even small-budded *Δcyk2* cells have abnormally wide necks (data not shown). Mutations in the septins and Myo1p also give rise to cells with wide bud necks (Flescher et al., 1993) (Lippincott, J., and R. Li, unpublished result). It is possible that Cyk2p, along with Myo1p and the septins, all localized at the incipient bud site, have an important structural role in determining the neck size early in the cell cycle.

A Role for Cyk2p in Stabilizing the Myo1 Ring during Contraction

Phenotypic analysis of *CYK2*-disrupted cells showed that Cyk2p plays an important, although not essential, role in cytokinesis, consistent with its localization at the bud neck. We did not observe any defect in the localization of actin or Myo1p to their destined structures in *Δcyk2* cells, but a severe defect was consistently observed during contraction of the Myo1 ring: although the brightness of the GFP–Myo1 fluorescence is maintained in the wild-type cells, it starts to diminish as soon as contraction initiates in *Δcyk2* cells. In some of the mutant cells observed, the fluorescence appears to diminish evenly in the ring, whereas in others the disassembly occurs unevenly. It was also apparent in many of the cells observed that cytokinesis was not accomplished after contraction.

The disassembly event was quantified by measuring the maximum fluorescence intensity of the GFP–Myo1 ring in cells where the disassembly occurred evenly in the ring. The maximum fluorescence intensity approximates the intensity of the pixels in focus and reflects the concentration of Myo1p in the ring. In the wild-type cells, it seems that there are two phases of fluorescence changes after the start of contraction: (*a*) a slight increase in fluorescence during contraction; and (*b*) a rapid loss of fluorescence after the ring becomes a dot (Fig. 6 *A*, panel *a*). However, rapid disassembly must also be occurring during the first phase, otherwise the intensity would have increased many fold since ring diameter decreased by approximately sixfold during contraction. Careful measurements of contractile ring volume have been made in *Arbacia* (sea urchin) eggs, which led to the same conclusion that contraction must be accompanied by disassembly (Schroeder, 1972).

The results discussed above may be in support of the solation–contraction coupling model, first proposed based on studies in *dictyostelium* extracts (Condeelis and Taylor, 1977; Taylor and Fechheimer, 1982). In this model, actin/myosin structures are prevented from contraction by extensive cross-linking in these structures (gelation). Solation by either a decrease in actin filament lengths or a decrease in the extent of the cross-linking would reduce the resistance against the sliding of actin and myosin II filaments and thereby stimulate contraction. In support of this model, it was observed that when fibroblast cells were treated with cytochalasin D, the stress fibers shorten rapidly, presumably by actomyosin-based contraction, with a concomitant loss of actin and myosin II from the fibers (Taylor and Fechheimer, 1982). Quantitative analysis was also carried out using an in vitro system consisting of a gel of actin and myosin II. The rate of contraction of this gel was inversely related to the amount of filamin, an F-actin cross-linking protein, present in the gel (Janson et al., 1991; Kolega et al., 1991).

If the solation–contraction model is correct, it is not difficult to predict that effective contraction, i.e., contraction that can pull a load such as the plasma membrane, must depend on a balance between solation and stabilization of the actomyosin-based structure (Fig. 8 *B*). Cyk2p may have a specialized role in the stabilization of the actomyosin ring during contraction. Thus, in the absence of Cyk2p, solation could occur to a greater extent, explaining the three times faster rate of contraction observed in the mutant than in the wild type. However, the rapid deterioration of the contractile ring could result in a loss of force and dissociation from the plasma membrane, explaining the frequent failure in cytokinesis. The cytokinesis defect of *Δcyk2* cells is more severe at elevated temperatures. This may be because the inward pulling force generated by actin and myosin is opposed by the turgor pressure that drives cell surface growth behind the actomyosin ring (Cosgrove, 1986; Bluemink and de Laat, 1973), and membrane trafficking occurs at a faster rate at 37°C (Novick et al., 1980).

Cyk2 May Have a Separate Function in Regulating Septin Localization

The observation that Cyk2p intimately associates with the septins by colocalization suggests that Cyk2p has an important interaction with the septins. In *Δcyk2* cells, the septins show normal distribution at the bud neck but exhibit a delay in delocalization from the old bud neck after the next round of budding. Therefore, Cyk2p may play a role in delocalizing the septin ring. It is not clear, however, to what extent the delay in septin delocalization contrib-

utes to the cytokinesis defect. Consistent with an ability to delocalize the septins from the bud neck, cells overexpressing Cyk2p lose the septin rings from the bud neck but form long septin filaments elsewhere in the cytoplasm. These aberrant septin filaments could be formed as a default due to the inability to localize to the bud neck, or alternatively, they might be promoted directly by the overexpressed Cyk2p. The former possibility would be more consistent with the defect in septin delocalization in *Δcyk2* cells and the result that Cyk2 rings are dependent on the septins. An ability of Cyk2p to remove septins from the bud neck must be tightly regulated, because Cyk2p colocalizes with the septins at the bud neck through most of the cell cycle. The overexpressed Cyk2p might override this regulation and displace the septins from the bud neck at any point in the cell cycle.

Functional Comparison of Cyk2 Homologues

Fission yeast cells deficient in cdc15p, the *S. pombe* homologue of Cyk2p, exhibit impaired assembly of the medial ring (Fankhauser et al., 1995; Balasubramanian et al., 1998). It is possible that this defect shares the same mechanistic cause with the defect in Myo1 ring stability in *Δcyk2* cells. In *S. pombe*, cdc15p colocalizes with the actomyosin ring starting from early M phase, and therefore it may be required for ring stabilization even before contraction. Cyk2p, on the other hand, colocalizes with the actomyosin ring late in the cell cycle and therefore may play a specialized role in ring stabilization during contraction. At this point, it is not clear whether the effect of cdc15p or Cyk2p on the stability of the actomyosin ring is mediated through actin or myosin II. Consistent with an interaction with actin, extended overexpression of Cyk2p results in the formation of aberrant F-actin aggregates at the bud neck (Fig. 7 *B*, *15 hr*), similar to those observed in *S. pombe* cells overexpressing cdc15p. A recent experiment showed that a cdc15 temperature sensitive mutant fails to accumulate actin patches at the septum after incubation at the nonpermissive temperature (Balasubramanian et al., 1998). We did not, however, observe any defect in actin patch distribution in *Δcyk2* cells. Thus, it is likely that Cyk2p and cdc15p have some differences in function.

Recently, imp2p, a cdc15p homologue was cloned in fission yeast (Demeter and Sazer, 1998). Imp2 is associated with the contractile ring in *S. pombe*. Interestingly, imp2p seems to be involved in the destabilization of the medial ring during septation, whereas Cyk2p appears to be important for the stabilization of the contractile ring (Demeter and Sazer, 1998).

PSTPIP, the mammalian homologue of Cyk2p, also localizes to the cleavage furrow, but its role in cytokinesis has not been investigated. PSTPIP has also been shown to localize to the cell cortex and stress fibers (Spencer et al., 1997). Because actin and myosin II are also present at the above locations, it is possible that PSTPIP has a general function in actomyosin-based contractility which is not restricted to cytokinesis in animal cells.

The authors are extremely grateful to A. Mallavarapu for providing custom software and help with video microscopy. We thank C. Field (Harvard Medical School) and J. Frazier (University of California, San Francisco, CA) for their gift of anti-Cdc3 antibodies, A. Straight (Harvard Medical School) for providing tubulin-GFP, D. Winter (Harvard Medical School) for providing Arp2–GFP, and J. Pringle (University of North Carolina, Chapel Hill, NC) for septin mutant strains. We are indebted to J. Swedlow (University of Dundee, Dundee, Scotland, UK), W. Prinz, and J. Yarrow (both from Harvard Medical School) for their help with three-dimensional deconvolution imaging and to S. Storms (Harvard Medical School) for computer assistance. We thank S. Shepard for preparation of media and solutions, and K. Shannon, D. Winter, T. Lechler, N. Tolliday, C. Field, A. Straight (all from Harvard Medical School), and F. Lippincott (Boston, MA) for support, thoughtful discussion, and critical reading of the manuscript.

This work was supported by a Funds for Discovery Award and the award from the Giovanni Armenise-Harvard Foundation to R. Li.

Received for publication 14 August 1998 and in revised form 28 October 1998.

References

Agard, D., Y. Hiraoka, P. Shaw, and J. Sedat. 1989. Fluorescence microscopy in three dimensions. *Methods Cell Biol.* 30:353–377.

Balasubramanian, M.K., D. McCollum, L. Chang, K.C.Y. Wong, N.I. Naqvi, X. He, S. Sazer, and K.L. Gould. 1998. Isolation and characterization of new fission yeast cytokinesis mutants. *Genetics.* 149:1265–1275.

Berben, G., J. Dumont, V. Gilliquet, P. Bolle, and F. Hilger. 1991. The YDp plasmid: a uniform set of vectors bearing versatile gene disruption cassettes for *Saccharomyces cerevisiae*. *Yeast*. 7:475–477.

Bi, E., P. Maddox, D.J. Lew, E.D. Salmon, J.N. McMillan, E. Yeh, and J.R. Pringle. 1998. Involvement of an actomyosin contractile ring in *Saccharomyces cerevisiae* cytokinesis. *J. Cell Biol.* 142:1301–1312.

Bluemink, J.G., and S.W. de Laat. 1973. New membrane formation during cytokinesis in normal and cytochalasin B-treated eggs of *Xenopus laevis*. I. Electron microscope observations. *J. Cell Biol.* 59:89–108.

Chang, F., and P. Nurse. 1996. Isolation and characterization of fission yeast mutants defective in the assembly and placement of the contractile actin ring. *J. Cell Sci.* 109:131–142.

Chang, F., D. Drubin, and P. Nurse. 1997. cdc12p, a protein required for cytokinesis in fission yeast, is a component of the cell division ring and interacts with profilin. *J. Cell Biol.* 137:169–182.

Condeelis, J., and D. Taylor. 1977. The contractile basis of amoeboid movement. V. The control of gelation, solation, and contraction in extracts from *Dictyostelium discoideum*. *J. Cell Biol.* 74:901–927.

Cosgrove, D. 1986. Biophysical control of plant cell growth. *Annu. Rev. Plant Physiol.* 37:377–405.

Demeter, J., and S. Sazer. 1998. imp2, a new component of the actin ring in the fission yeast *Schizosaccharomyces pombe*. *J. Cell Biol.* 143:415–427.

Drubin, D.G., K.G. Miller, and D. Botstein. 1988. Yeast actin-binding proteins: evidence for a role in morphogenesis. *J. Cell Biol.* 107:2551–2561.

Evan, G.I., G.K. Lewis, G. Ramsay, and J.M. Bishop. 1985. Isolation of monoclonal antibodies specific for human c-*myc* proto-oncogene product. *Mol. Cell. Biol.* 5:3610–3616.

Fankhauser, C., A. Reymond, L. Cerutti, S. Utzig, K. Hofmann, and V. Simanis. 1995. The *S. pombe* cdc15 gene is a key element in the reorganization of F-actin at mitosis. *Cell*. 82:435–444.

Fishkind, D.J., and Y.L. Wang. 1995. New horizons for cytokinesis. *Curr. Opin. Cell Biol.* 7:23–31.

Flescher, E., K. Madden, and M. Snyder. 1993. Components required for cytokinesis are important for bud site selection in yeast. *J. Cell Biol.* 122:373–386.

Frazier, J.A., M.L. Wong, M.S. Longtine, J.R. Pringle, M. Mann, T.J. Mitchison, and C. Field. 1998. Polymerization of purified yeast septins: evidence that organized filament arrays may not be required for septin function. *J. Cell Biol.* 143:737–749.

Gould, K.L., and V. Simanis. 1997. The control of septum formation in fission yeast. *Genes Dev.* 11:2939–2951.

Guthrie, C., and G.R. Fink. 1991. Guide to Yeast Genetics and Molecular Biology. Methods in Enzymology. Academic Press, New York. 194 pp.

Haarer, B.K., and J.R. Pringle. 1987. Immunofluorescence localization of the *Saccharomyces cerevisiae CDC12* gene product to the vicinity of the 10-nm filaments in the mother-bud neck. *Mol. Cell Biol.* 7:3678–3687.

Hartwell, L.H. 1971. Genetic control of cell division cycle in yeast. *Exp. Cell Res.* 69:265–276.

Janson, L., J. Kolega, and D. Taylor. 1991. Modulation of contraction by gelation/solation in a reconstituted motile model. *J. Cell Biol.* 114:1005–1015.

Kaiser, C., S. Michaelis, and A. Mitchell. 1994. Methods in Yeast Genetics. Cold Spring Harbor Laboratory Press, Cold Spring Harbor, NY. 234 pp.

Kim, H.B., B.K. Haarer, and J.R. Pringle. 1991. Cellular morphogenesis in the *Saccharomyces cerevisiae* cell cycle: localization of the *CDC3* gene product and the timing of events at the budding site. *J. Cell Biol.* 112:535–544.

Kinoshita, M., S. Kumar, A. Mizoguchi, C. Ide, A. Kinoshita, T. Haraguchi, Y. Hiraoka, and M. Noda. 1997. Nedd5, a mammalian septin, is a novel cytoskeletal component interacting with actin-based structures. *Genes Dev.* 11:

1535–1547.
Kolega, J., L.W. Janson, and D.L. Taylor. 1991. The role of solation-contraction coupling in regulating stress fiber dynamics in nonmuscle cells. *J. Cell Biol.* 114:993–1003.
Lippincott, J., and R. Li. 1998. Sequential assembly of myosin II, an IQGAP-like protein, and filamentous actin, to a ring structure involved in budding yeast cytokinesis. *J. Cell Biol.* 140:355–366.
Longtine, M.S., D.J. DeMarini, M.L. Valencik, O.S. Al-Awar, H. Fares, C. De Virgilio, and J.R. Pringle. 1996. The septins: roles in cytokinesis and other processes. *Curr. Opin. Cell Biol.* 8:106–119.
Maupin, P., C. Phillips, R. Adelstein, and T. Pollard. 1994. Differential localization of myosin-II isozymes in human cultured cells and blood cells. *J. Cell Sci.* 107:3077–3090.
Novick, P., C. Field, and R. Schekman. 1980. Identification of 23 complementation groups required for posttranslational events in the yeast secretory pathway. *Cell*. 21:205–215.
Pringle, J. 1991. Staining of bud scars and other cell wall chitin with calcofluor. *In* Guide to Yeast Genetics and Molecular Biology. Vol. 194. C. Guthrie and G. Fink, editors. Academic Press, San Diego, CA. 732–735.
Satterwhite, L.L., and T.D. Pollard. 1992. Cytokinesis. *Curr. Opin. Cell Biol.* 4:43–52.
Schroeder, T.E. 1972. The contractile ring. II. Determining its brief existence, volumetric changes, and vital role in cleaving *Arbacia* eggs. *J. Cell Biol.* 53: 419–434.
Schroeder, T.E. 1990. The contractile ring and furrowing in dividing cells. *Ann. NY Acad. Sci.* 582:78–87.
Sherman, F., G. Fink, and C. Lawrence. 1974. Methods in Yeast Genetics. Cold Spring Harbor Laboratory Press, Cold Spring Harbor, NY. 186 pp.
Spencer, S., D. Dowbenko, J. Cheng, W. Li, J. Brush, S. Utzig, V. Simanis, and L.A. Lasky. 1997. PSTPIP: a tyrosine phosphorylated cleavage furrow-associated protein that is a substrate for a PEST tyrosine phosphatase. *J. Cell Biol.* 138:845–860.
Straight, A.F., W.F. Marshall, J.W. Sedat, and A.W. Murray. 1997. Mitosis in living budding yeast: anaphase A but no metaphase plate. *Science*. 277:574–578.
Taylor, D., and M. Fechheimer. 1982. Cytoplasmic structure and contractility. The solation-contraction coupling hypothesis. *Phil. Trans. Soc. Lond. B. Biol. Sic.* 299:185–197.
Verkhovsky, A., and G. Borisy. 1993. Non-sarcomeric mode of myosin-II organization in the fibroblast lamellum. *J. Cell Biol*. 123:637–652.
Waddle, J.A., T.S. Karpova, R.H. Waterson, and J.A. Cooper. 1996. Movement of cortical actin patches in yeast. *J. Cell Biol.* 132:861–870.
Watts, F.Z., G. Shiels, and E. Orr. 1987. The yeast *MYO1* gene encoding a myosin-like protein required for cell division. *EMBO (Eur. Mol. Biol. Organ.) J.* 6:3499–3505.